# Phospholamban Decreases the Energetic Efficiency of the Sarcoplasmic Reticulum Ca Pump*

**Thomas R. Shannon‡, Guoxiang Chu§, Evangelia G. Kranias§, and Donald M. Bers‡¶**

*From the ‡Department of Physiology, Loyola University Chicago, Maywood, Illinois 60153 and the
§Department of Pharmacology and Cell Biophysics, University of Cincinnati, Cincinnati, Ohio 45267*

We tested the hypothesis that increased Sarcoplasmic reticulum (SR) Ca content ($[Ca]_{SRT}$) in phospholamban knockout mice (PLB-KO) is because of increased SR Ca pump efficiency defined by the steady-state SR [Ca] gradient. The time course of thapsigargin-sensitive ATP-dependent $^{45}$Ca influx into and efflux out of cardiac SR vesicles from PLB-KO and wild-type (WT) mice was measured at 100 nM free [Ca]. We found that PLB decreased the initial SR Ca uptake rate (0.13 *versus* 0.31 nmol/mg/s) and decreased steady-state $^{45}$Ca content (0.9 *versus* 4.1 nmol/mg protein). Furthermore, at similar total SR [Ca], the pump-mediated Ca efflux rate was higher in WT (0.065 *versus* 0.037 nmol/mg/s). The pump-independent leak rate constant ($k_{leak}$) was also measured at 100 nM free [Ca]. The results indicate that $k_{leak}$ was <1% of pump-mediated backflux and was not different among nonpentameric mutant PLB (PLB-C41F), WT pentameric PLB (same expression level), and PLB-KO. Therefore differences in passive SR Ca leak cannot be the cause of the higher thapsigargin-sensitive Ca efflux from the WT membranes. We conclude that the decreased total SR [Ca] in WT mice is caused by decreased SR Ca influx rate, an increased Ca-pump backflux, and unaltered leak. Based upon both thermodynamic and kinetic analysis, we conclude that PLB decreases the energetic efficiency of the SR Ca pump.

The SR[1] Ca pump is an important cellular protein that

¶ To whom correspondence should be addressed: Dept. of Physiology, Loyola University Medical Center, 2160 S. First Ave., Maywood, IL 60153. Tel.: 708-216-1018; Fax: 708-216-6308; E-mail: dbers@luc.edu.

[1] The abbreviations used are: SR, sarcoplasmic reticulum; $\Delta G_{ATP}$, free energy in the form of ATP; $B_{max}$, maximal binding capacity; $B_{max\text{-}SR}$, maximal intra-SR Ca binding capacity; $[Ca]_c$, [Ca] outside; $[Ca]_{SR}$, free SR [Ca]; $[Ca]_{SRT}$, total SR [Ca]; $[Ca]_{SRT+efl}$, efflux buffer-sensitive $[Ca]_{SRT}$; $[Ca]_{SRT\text{-}efl}$, efflux buffer-insensitive $[Ca]_{SRT}$; $[Ca]_{SRT\text{-}SS}$, steady-state $[Ca]_{SRT}$; $[Ca]_T$, total [Ca] outside; PLB, phospholamban; PLB-C41F, nonpentameric mutant mice; $\Delta G_{SRCa}$, free energy used by the SR Ca pump to generate the free SR [Ca] gradient; $E_{pump}$, SR Ca pump efficiency; $k_{efl}$, time constant of $^{45}$Ca efflux; $n$, Hill coefficient; $nf$, Hill coefficient of unidirectional forward flux; $nr$, Hill coefficient of unidirectional backward flux; $k_{inf}$, time constant of $^{45}$Ca influx; $J_{leak}$, SR leak flux; $J_{pump}$, net SR Ca pump flux; $J_{pumpf}$, forward SR Ca pump flux; $J_{pumpr}$, reverse SR Ca pump flux; $J_{SR}$, SR Ca flux; $K_d$, ion binding affinity; $K_{d\text{-}SR}$, SR Ca binding affinity; $K_{Ca}$, $[Ca]_c$ concentration at half-maximal net SR Ca pump rate; $K_{Ca\text{-}f}$, $[Ca]_c$ at half-maximal forward SR Ca pump rate; $K_{Ca\text{-}r}$, $[Ca]_c$ at half-maximal reverse SR Ca pump rate; $k_{leak}$, SR Ca leak rate constant; WT, wild-type mice; PLB-KO, phospholamban knockout mice; PLB-70, mice expressing WT PLB against a PLB-KO background; Thg, thapsigargin; $V_{max}$, maximal net

transduces the energy stored in cytosolic ATP ($\Delta G_{ATP}$) into energy that is stored as a [Ca] gradient across the SR membrane ($\Delta G_{SRCa}$). The pump establishes this gradient at steady-state through a balance of the following 3 fluxes: an SR Ca pump-dependent influx balanced by a pump-dependent efflux (or "backflux") and a passive leak flux (mediated by the ryanodine receptor or other pathways).

Backflux is a unidirectional flux that results from reversal of the SR Ca pump in the forward mode. High Ca within the SR is transported through the pump back into the cytosol, and ATP can be made from ADP and inorganic phosphate as has been demonstrated directly in SR membrane vesicles (1–4). Backflux has also been described in both digitonin-permeabilized isolated cardiac myocytes (5) and in isolated myocytes under whole-cell voltage clamp (6).

Phospholamban (PLB) is an important regulator of the SR Ca pump. In the unphosphorylated state it associates with the SR Ca pump to inhibit its activity. This inhibition can be relieved through phosphorylation by protein kinase A and/or Ca-calmodulin-dependent protein kinase (7, 8). Although it is well established that PLB inhibits the forward mode of SR Ca transport by increasing the forward $K_{Ca}$ ($K_{Ca\text{-}f}$) to higher [Ca], the effects of PLB on reverse SR Ca-ATPase and $K_{Ca}$ ($K_{Ca\text{-}r}$) are unknown. This becomes an important issue, especially in the case where the Ca pump approaches thermodynamic equilibrium, as may be the case in intact myocytes under some conditions (9). That is, the forward and reverse Ca flux can reach the point where they are equal and opposite, and the [Ca] gradient is maximal at about 7000:1 (10). If PLB shifts $K_{Ca\text{-}f}$ without shifting $K_{Ca\text{-}r}$ by a comparable amount, the maximal [Ca] gradient that the SR Ca pump can generate may change, and this could alter the energetic efficiency of the pump.

PLB coexists in the cardiac myocyte in both a monomeric and pentameric form. The pentameric form has been reported to form a channel that may mediate Ca leak from the SR (11, 12).

In this report we measure forward and reverse Ca pump flux and also pump-independent leak in SR vesicles from wild-type (WT) mice, phospholamban knockout mice (PLB-KO), and mice that express equal amounts of either wild-type PLB (PLB-70) or nonpentamer-forming mutant PLB (PLB-C41F) upon a knockout background. Nonpump-mediated Ca leak was not different among these groups, which does not support any significant role for a PLB-mediated leak under our conditions.

We hypothesize that PLB inhibits SR Ca pump influx at the same time that it stimulates SR Ca pump backflux. Such an effect would result in a decreased $\Delta G_{SRCa}$ and decreased SR Ca pump energetic efficiency. The data in WT, PLB-KO, and PLB-70 membranes all support this hypothesis.

SR Ca pump rate; $V_{maxf}$, maximal forward SR Ca pump rate; $V_{maxr}$, maximal reverse SR Ca pump rate; BAPTA, 1,2-bis(2-aminophenoxy)ethane-$N,N,N',N'$-tetraacetic acid; Mops, 4-morpholinepropanesulfonic acid; ANOVA, analysis of variance.

## MATERIALS AND METHODS

All chemicals were from Sigma, except as indicated. Mathematical data manipulation was performed using Lotus 1–2–3 (Lotus Development Corp., Cambridge, MA) and Excel (Microsoft Corp., Seattle, WA). Nonlinear regression fits and statistics were done with GraphPad (iSi Software, Philadelphia, PA).

*SR Ca Influx and Backflux Assay*—For the purposes of this paper the efficiency of the SR Ca pump is defined as follows:

$$Eft_{pump} = \frac{\Delta G_{SRCa} \cdot 100}{\Delta G_{ATP}} \qquad (Eq. 1)$$

where $\Delta G_{ATP}$ is the free energy stored in the form of ATP in the cytosol or 59 kJ/mol (13) and $\Delta G_{SRCa}$ is the free energy required by the pump to establish the SR [Ca] gradient. This is defined as follows:

$$\Delta G_{SRCa} = 2RT \cdot \ln \frac{[Ca]_{SR}}{[Ca]_c} \qquad (Eq. 2)$$

where $[Ca]_{SR}$ is free SR Ca and $[Ca]_{SR}/[Ca]_c$ is the free SR Ca gradient. Therefore when the pump generates a higher SR [Ca] gradient, it is operating at a higher energetic efficiency. In this paper we measure $[Ca]_{SRT}$ (and relate it to $[Ca]_{SR}$) in SR membrane vesicles at 100 nM $[Ca]_c$ as a measure of the SR [Ca] gradient.

*Experimental Procedures*—PLB-KO, PLB-70, and WT mice were anesthetized with 0.25 mg of pentobarbital/g of body weight. Thoracotomy was performed, and hearts were removed, cannulated via the aorta, and perfused with 5 ml of 10 mM caffeine, 10 mM EGTA, normal tyrode. Normal tyrode consisted of (in mM) 140 NaCl, 4 KCl, 10 glucose, 5 HEPES, and 1 MgCl$_2$, pH 7.4, with NaOH. Hearts were then perfused with 15 ml of 0.5 mM BAPTA in (in mM) 140 sucrose, 70 KCl, 40 HEPES, pH 7.2 (membrane buffer). Subsequently, the ventricular tissue was separated from the rest of the heart and put into 0.5 BAPTA membrane buffer, minced, and homogenized with two 15-s pulses of a polytron homogenizer (Brinkmann Instruments, Inc., Westbury, NY). This procedure depletes the membranes of endogenous Ca. The membranes that resulted were centrifuged at 100,000 × g, resuspended in 1 ml 0.5 BAPTA, 100 μg/ml aprotinin, 100 μg/ml leupeptin, 0.5 ryanodine, and 20 μM digitonin in membrane buffer, and glass-Teflon homogenized.

The membranes were split into two portions. One was treated with 25 nmol/mg thapsigargin (Thg) and the other with Me$_2$SO vehicle. The membranes were incubated for 20 min at room temperature to allow ryanodine and thapsigargin binding and were then put on ice.

Triplicate incubates were set up for plus and minus Thg groups. Each incubate contained 86 μl of uptake buffer. MgATP (4 μl, 100 mM stock) and 10 μl of membranes (~5 mg/ml) were beaded on the side of the test tube, and the assay for each time point was begun by vortexing, thus washing the ATP and the membranes into the incubate. The incubates contained (final concentration in mM during incubation) 0.69 MgCl$_2$, 0.5 BAPTA, 0.151 CaCl$_2$ (100 nM $[Ca]_c$, 100–200 μCi of $^{45}$Ca), 4 MgATP, 10 μg/ml aprotinin, 10 μg/ml leupeptin, 14 sucrose, 127 KCl, 40 HEPES, pH 7.2. Phosphocreatine (12.5) and 5 units/ml creatine phosphokinase were present to regenerate ATP. Mitochondrial Ca uptake was inhibited by 2 μM ruthenium red and 4 μM oligomycin. Digitonin (20 μM) inhibited sarcolemmal Ca uptake, and ryanodine receptors were blocked by 0.5 mM ryanodine. Uptake was stopped with an ice-cold solution (in mM) of 1 EGTA, 200 KCl, 20 Mops, Tris to pH 7.4 (stop solution). The incubates were vacuum-filtered through Whatman GF/C glass fiber filters (Fisher Scientific, Pittsburgh, PA). The tubes were washed 3×, and the filter was washed an additional 2× with stop solution.

Membranes were allowed to take up Ca for 0, 10, 20, 30, 60, and 90 s, thus forming the uptake part of the curve (see Fig. 2). The backflux part of the curve was constructed from incubates that were allowed to take up Ca for 90 s, at which point an efflux buffer was added. Efflux buffer consisted of (final concentration in mM during incubation) 50 EGTA, 17.1 CaCl$_2$ (100 nM $[Ca]_c$), 40 HEPES, pH 7.2. This solution caused $^{45}$Ca efflux while holding $[Ca]_c$ at 100 nM and reducing extracellular $^{45}$Ca specific activity 100-fold. The indicated time points were taken after the addition of efflux buffer. Membrane protein concentration was determined using the Bio-Rad total protein assay reagent kit (Bio-Rad Laboratories, Hercules, CA).

*Data Analysis*—The influx part of the experiment was fit with a rising exponential function,

$$[Ca]_{SRT} = [Ca]_{(SRT-SS)} (1 - \exp(-k_{inf} \cdot t)) \qquad (Eq. 3)$$

where $k_{inf}$ is the rate constant and $t$ is time. Steady-state $[Ca]_{SRT}$ ($[Ca]_{SRT-SS}$) was therefore the plateau of the relationship. Note that the described data are "efflux-sensitive" uptake. We found that a varying percentage of the total Ca taken up did not come out of the membranes upon addition of efflux buffer. We therefore characterized the kinetics of the SR Ca pump only in terms of Ca available for transport into and out of the membranes.

The initial rate of uptake was determined as the derivative of this function at $t = 0$.

$$J_{SR} = \frac{d[Ca]_{SRT}}{dt} = k_{inf} \cdot [Ca]_{(SRT-SS)} \cdot \exp(-k_{inf} \cdot t) \qquad (Eq. 4)$$

Similarly, the efflux part of the time course was described with an exponential decay,

$$[Ca]_{SRT} = [Ca]_{(SRT+efl)} \cdot \exp(-k_{efl} \cdot t) + [Ca]_{(SRT-efl)} \qquad (Eq. 5)$$

where $[Ca]_{SRT+efl}$ is efflux buffer-sensitive $[Ca]_{SRT}$, and $[Ca]_{SRT-efl}$ is efflux buffer-insensitive $[Ca]_{SRT}$ (*i.e.* see Fig. 2, bottom plateau of the curve). $k_{inf}$ is the rate constant, and $t$ is the time from dilution. The rate of efflux at identical $[Ca]_{SRT+efl}$ (0.8 nmol/mg) in all groups was determined from the following derivative:

$$J_{SR} = -k_{efl} \cdot [Ca]_{(SRT+efl)} \cdot \exp(-k_{efl} \cdot t) \qquad (Eq. 6)$$

where $t$ is the time from dilution to $[Ca]_{SRT-efl} = 0.8$ nmol/mg.

*Calculation of $\Delta G_{SRCa}$ from Ca Uptake Kinetics*—The initial rate of $^{45}$Ca uptake when $[Ca]_{SR} = 0$ is described by the classic Hill equation,

$$J_{pumpf} = \frac{V_{max}}{1 + \left(\frac{K_{Ca-f}}{[Ca]_c}\right)^n} \qquad (Eq. 7)$$

where $J_{pumpf}$ is the forward pump rate and $V_{max}$, $K_{Ca-f}$, and $n$ are the maximal velocity, $[Ca]_c$ at half-maximal velocity, and the Hill coefficient in the forward direction, respectively. We set $n$ to 2, $K_{Ca-f}$ to 0.25, and 0.14 for WT and PLB-KO, respectively (as measured by Frank, *et al.* (14)). Given these parameters and $J_{pumpf}$, $V_{max}$ was determined.

The rate of backflux at steady-state was also determined by using Equation 6, where $t = 0$ (*i.e.* the rate when excess $^{40}$Ca is added; see Fig. 2). This rate is described by the following:

$$J_{pumpr} = \frac{V_{max}\left(\frac{[Ca]_{SR}}{K_{(Ca-r)}}\right)^n}{1 + \left(\frac{[Ca]_c}{K_{Ca-f}}\right)^n + \left(\frac{[Ca]_{SR}}{K_{Ca-r}}\right)^n} \qquad (Eq. 8)$$

where $J_{pumpr}$ is the unidirectional reverse pump rate and $K_{Ca-r}$ has its usual meaning for the reverse pump rate. This is a special case of the generic reversible equation,

$$J_{pump} = \frac{V_{maxf}\left(\frac{[Ca]_c}{K_{Ca-f}}\right)^{nf} - V_{maxr}\left(\frac{[Ca]_{SR}}{K_{Ca-r}}\right)^{nr}}{1 + \left(\frac{[Ca]_c}{K_{Ca-f}}\right)^{nf} + \left(\frac{[Ca]_{SR}}{K_{Ca-r}}\right)^{nr}} \qquad (Eq. 9)$$

where $V_{maxf} = V_{maxr}$ and $nf = nr$. For $^{45}$Ca efflux, the left term in the numerator is zero, giving Equation 8. Given $J_{pumpr}$ and the $V_{max}$ above, the $K_{Ca-r}$ can be inferred from Equation 8.

At steady-state $J_{pump}$ is zero, so the numerator of Equation 9 is zero, and this reduces to the Haldane relationship.

$$\frac{[Ca]_{SR}}{[Ca]_c} = K_{eq} = \frac{K_{Ca-r}}{K_{Ca-f}} \qquad (Eq. 10)$$

Combining with Equation 2, we arrive at Equation 11.

$$\Delta G_{SRCa} = 2RT \cdot \ln \frac{K_{Ca-r}}{K_{Ca-f}} \qquad (Eq. 11)$$

Thus, if we know $K_{Ca-f}$ and derive $K_{Ca-r}$ from Equation 8 the $\Delta G_{SRCa}$ can be inferred.

*SR Ca Leak*—Membranes from PLB-KO, PLB-70, and PLB-C41F mice were prepared as above except 30 μM EGTA, 10 μg/ml aprotinin, and 10 μg/ml leupeptin, 140 KCl, 40 HEPES, pH 7.4 was used for perfusion, homogenization, and resuspension instead of BAPTA.

The protocol for measuring passive SR Ca leak from the membranes is illustrated in Fig. 1A. Mouse membranes were added to a cuvette

with stirring at a final concentration of ~1–2 mg/ml. Also present were (final concentrations) EGTA (30 $\mu$M), MgCl$_2$ (1 mM free), the protease inhibitors aprotinin and leupeptin (10 $\mu$g/ml), oligomycin (2 $\mu$M) and ruthenium red (2 $\mu$M) to inhibit mitochondrial uptake, and 0.5 mM ryanodine to block ryanodine receptors. $[Ca]_c$ was measured with 2 $\mu$M indo-1 (Molecular Probes, Eugene, OR). An 8100 series spectrofluorometer (Spectronic Instruments, Rochester, NY) was used to excite the indo-1 at 355 nm. Fluorescence emission at 400 and 470 nm was measured. The 400:470 ratio was converted to $[Ca]_c$ using the Grynkiewicz equation (9, 15).

Uptake was started by 4 mM ATP addition. ATP was regenerated with 5 units/ml creatine phosphokinase and 12.5 mM phosphocreatine. EGTA or Ca was added such that a plateau was reached at ~100 nM $[Ca]_c$. $[Ca]_c$ gradually rose after 10 nmol/mg Thg was added until the SR Ca pump was completely blocked. Passive leak continued until the SR was empty of Ca.

The leak rate constant (see below) was used to characterize the leak in the different groups of membranes. $[Ca]_c$ was converted to total Ca ($[Ca]_T$) using known Ca binding constants for all buffers within the cuvette (see Table I). These binding constants were collected from the literature, and nearly all of the endogenous affinity constants come from *in vitro* measurements where physiological intracellular conditions were simulated (normal ionic strength and pH value), usually at room temperature.

Exogenous EGTA and indo-1 are overwhelmingly the dominant Ca buffering species accounting for >98% of the Ca bound ($\geq$32 $\mu$M *versus* ~0.3 $\mu$M). Fortunately these are the buffers that we know the most about and of which we can be most sure. Constants for EGTA in particular were fully corrected for ionic strength and pH value using the Maxchelator program (see Ref. 16; free for download on the World Wide Web).

Referenced values were converted from nmol/mg to $\mu$mol/liter cytosol using the conversion factors 0.4 liter of cell volume/kg of wet weight, 120 mg of homogenate protein/g of wet weight (17) and a measured value of 0.312 mg of membranes/mg of homogenate.

Therefore for each time point in Fig. 1A, we know $[Ca]_c$ and $[Ca]_T$. The difference between the $[Ca]_T$ before Thg and $[Ca]_T$ after all of the Ca has leaked out of the SR is the $[Ca]_{SRT}$ just prior to Thg addition. Because we know how much Ca leaks out of the SR during the experiment, we can now calculate $[Ca]_{SRT}$ at each time point as the amount of Ca that hasn't leaked out yet.

Given $[Ca]_{SRT}$ and the SR Ca buffering parameters, $[Ca]_{SR}$ can be calculated. SR volume was assumed to be 3% of cellular volume (18, 19). $[Ca]_{SRT}$ was converted to $[Ca]_{SR}$ using the following relationships.

$$[Ca]_{SRT} = [Ca \cdot L]_{SR} + [Ca]_{SR} \qquad (\text{Eq. 12})$$

$$[Ca \cdot L]_{SR} = \frac{B_{max-SR} \cdot [Ca]_{SR}}{K_{d-SR} + [Ca]_{SR}} \qquad (\text{Eq. 13})$$

$B_{max-SR}$ and $K_{d-SR}$ have been previously determined to be 14 mmol/liter of SR and 638 $\mu$M, respectively (10). Equation 13 was substituted into Equation 12, and $[Ca]_{SR}$ as a function of $[Ca]_{SRT}$ was calculated from the quadratic solution of the result.

The leak rate ($J_{leak}$) is the change in $[Ca]_T$ over time and is assumed to be proportional to the concentration difference ($[Ca]_{SR} - [Ca]_c$),

$$J_{leak} = k_{leak}([Ca]_{SR} - [Ca]_c) \qquad (\text{Eq. 14})$$

where $k_{leak}$ is a rate constant of leak flux, determined by linear regression of leak flux data (see Fig. 1B; *gray line*).

## RESULTS

*PLB Dependence of SR Ca Leak*—There are two primary routes of Ca efflux from the SR when the ryanodine receptors are blocked with high ryanodine (as is the case with all of the experiments here). These are backflux (1–6) and passive SR Ca leak across the membrane. To measure $E_{pump}$ with and without PLB we must first determine the extent to which passive leak rate contributes to SR Ca efflux in our system.

Fig. 1A shows the protocol that we used to measure this leak rate. When $[Ca]_c$ was ~100 nM, Thg (25 nmol/mg) was added. Thg forms a dead-end complex with the SR Ca pump (20) thus inhibiting both SR Ca influx and backflux through the pump. $[Ca]_c$ gradually rose until the SR Ca pump was completely blocked. Passive leak continued until the SR was empty of Ca.
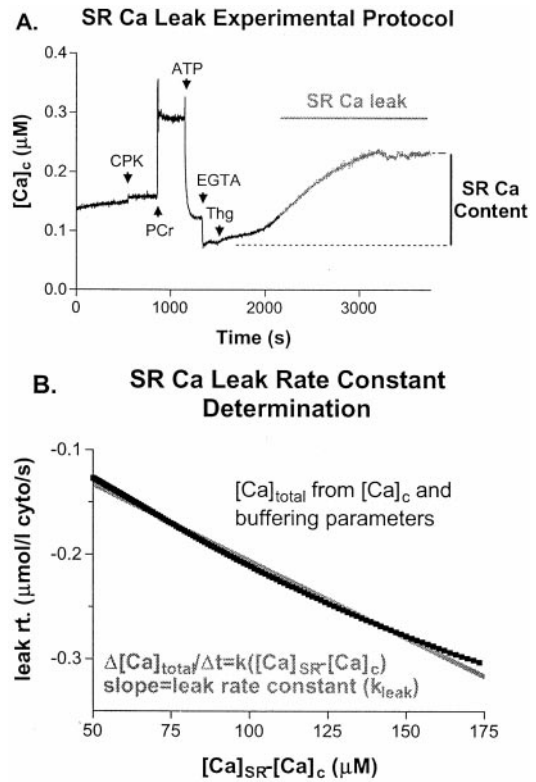


FIG. 1. **Protocol for measuring passive SR Ca leak from the membranes.** *A*, 1–2-mg/ml membranes were added to a cuvette with stirring. The cuvette contained (final concentrations) 30 $\mu$M EGTA, 1 mM free MgCl$_2$, 10 $\mu$g/ml aprotinin, 10 $\mu$g/ml leupeptin, 2 $\mu$M oligomycin, 2 $\mu$M ruthenium red, and 0.5 mM ryanodine. Fluorescence outside the vesicles was measured with 2 $\mu$M indo-1 and converted to $[Ca]_c$. ATP (4 mM) was added to start uptake. Creatine phosphokinase (*PCr*; 5 units/ml) and 12.5 mM phosphocreatine regenerated ATP (note the increased fluorescence upon phosphocreatine addition because of Ca contamination). EGTA or Ca was added such that a plateau was reached at approximately 100 nM $[Ca]_c$. Thg (25 nmol/mg protein) was added, and $[Ca]_c$ rose until the SR Ca pump was completely blocked. Passive leak continued until the SR was empty of Ca. $[Ca]_c$ was converted to total Ca using known Ca binding constants for all buffers within the cuvette (Table I). Endogenous affinity constants come from *in vitro* measurements where physiological intracellular conditions were simulated as nearly as possible (normal ionic strength and pH value) usually at room temperature. Exogenous EGTA and indo-1 are far and away the dominant Ca buffering species accounting for >98% of the Ca bound. $[Ca]_{SRT}$ was computed as Ca at the end of the leak minus Ca before Thg allowing calculation of $[Ca]_{SRT}$ and $[Ca]_{SR}$ for all times. Thg, $B$, $k_{leak}$ was determined as the slope of the relationship between leak rate and ($[Ca]_{SR} - [Ca]_c$) (6). The *gray line* is the regression through the data (*black points*).

$[Ca]_T$ was computed at each time point using known Ca binding constants (Table I). $[Ca]_{SRT}$ was computed as $[Ca]_T$ at the end of the leak minus $[Ca]_T$ before Thg, and both $[Ca]_{SRT}$ and $d[Ca]_{SRT}/dt$ could be calculated for each time point. $[Ca]_{SR}$ was calculated using Equations 12 and 13 (10). The slope of the relationship between the leak flux ($J_{leak}$) and the free Ca difference across the SR membrane is $k_{leak}$ (Fig. 1B).

The following three groups of mice were compared: 1) transgenic mice that expressed only mutant nonpentamer-forming PLB (Ref. 21; PLB-C41F), 2) PLB-KO, and 3) PLB-70 (mice that express WT PLB at the same level as the mutant PLB is expressed in PLB-C41F). There was no significant difference in SR Ca leak between the PLB-C41F group, the PLB-70 group, and the PLB-KO group (0.058 $\pm$ 0.011 *versus* 0.061 $\pm$ 0.010 *versus* 0.045 $\pm$ 0.006/min, Student's *t* test, $p > 0.05$, $n = 6$).

We conclude that passive SR Ca leak is unchanged in mice containing mutant or wild-type PLB or in PLB-KO. Further-

TABLE I
*Cuvette Ca Buffering Parameters*

Although all are accounted for, note that EGTA and indo-1 account for the majority of the buffering capacity.

| Buffer | $B_{\max}$ | $K_d$ | Ref. |
|---|---|---|---|
| | | $\mu M$ | |
| SR Ca pump | 0.1576 $\mu$M | 0.6 | 39 |
| Sarcolemma | 0.14 $\mu$M | 13 | 40 |
| Membrane/high | 0.05 $\mu$M | 0.3 | 41 |
| EGTA · Ca | $\geq$30 $\mu$M | 0.173 | 42 |
| EGTA · Mg | $\geq$30 $\mu$M | 23300 | 42 |
| Indo-1 | 2 $\mu$M | 0.45 | 43 |

more, there was no evidence of SR Ca leak through a pentameric PLB channel under these conditions.

*SR Ca Influx and Backflux Assay*—Fig. 2A shows the protocol for measuring unidirectional SR Ca fluxes along with a typical experiment. $^{45}$Ca uptake is started with the addition of ATP and ventricular membranes to the uptake medium as described under "Materials and Methods." Incubates were filtered at the indicated times to measure $[Ca]_{SRT}$. At 90 s excess nonradioactive $^{40}$Ca buffered with 50 mM EGTA was added. The high Ca/EGTA concentration diluted the $^{45}$Ca to negligible levels while maintaining a $[Ca]_c$ of 100 nM. Under this condition, unidirectional SR $^{45}$Ca efflux took place. Note that the actual $[Ca]_{SRT}$ and the fluxes at steady-state have not changed here. The backflux has only been "uncovered" by the dilution of $^{45}$Ca outside the vesicles. This is demonstrated in Fig. 2B, where Ca flux rates were calculated from SR Ca content data as in Fig. 2A. In this case mean kinetic parameters were taken from the mean PLB-KO data (see below). Fig. 2A (*dashed line*) shows that although the $[^{45}Ca]$ has changed, $[Ca]_c$ and $[Ca]_{SRT}$ (and $[Ca]_{SR}$) have not. The $^{45}$Ca efflux gives a measure of the unidirectional backflux at steady-state, but the net total Ca flux is still zero. Also note the rapid loss of $^{45}$Ca compared with the leak in Fig. 1A (translated into the *gray dashed line* in Fig. 2A). Therefore nearly all of this $^{45}$Ca efflux is backflux through the SR Ca pump (Fig. 2A).

As can be seen in Fig. 3A, $^{45}$Ca began to accumulate in the SR immediately upon ATP and membrane addition in both WT and PLB-KO. $[Ca]_{SRT}$ came nearly to steady-state where Ca influx and efflux are equal by 90 s. $[Ca]_{SRT-SS}$ as determined by Equation 3 in WT was ~25% of that in PLB-KO (0.9 *versus* 4.1 nmol/mg of protein). This important result may reflect a lower SR [Ca] gradient and therefore a lower $\Delta G_{SRCa}$ (Equation 2) at steady-state.

Note that in some experiments, we found a varying percentage of the total Ca taken up did not come out of the membranes upon addition of efflux buffer (the *nonzero plateau* in Fig. 3B). This Ca appears to be pump-insensitive. Characterization of the kinetics of the SR Ca pump is therefore only in terms of Ca that was available for both uptake and efflux from the membranes. $[Ca]_{SRT-SS}$ is therefore the plateau in Fig. 3A minus the efflux-insensitive Ca (*i.e.* the *plateau* in Fig. 3B). Note that this treatment is conservative in that it tends to minimize differences between WT and PLB-KO.

From the higher $[Ca]_{SRT}$ in PLB-KO we conclude that the efficiency of SR Ca uptake is lower in the presence of PLB (Equation 1). The only alternatives would be (1) a difference in leak flux (not the case, see above) or (2) different intra-SR Ca buffering. The latter is highly unlikely, because the calsequestrin concentration is the same in PLB-KO and WT mice (22), and the concentration would have to be five times higher to explain the results. These results are also consistent with findings of much higher SR Ca load in PLB-KO intact myocytes (23).

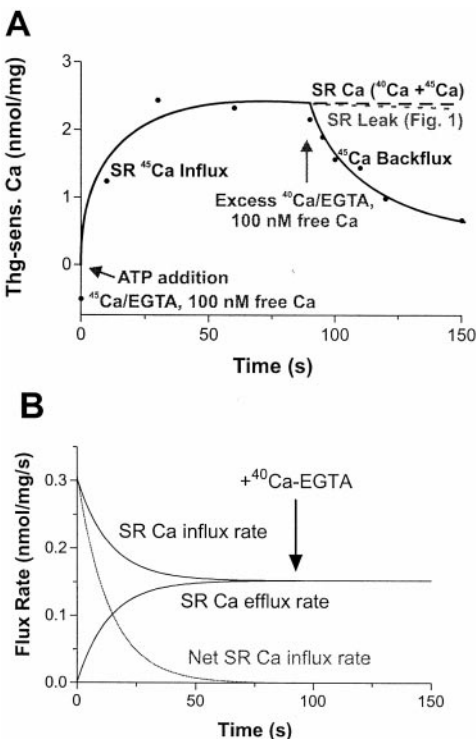Having examined the raw data, we can now further charac-



FIG. 2. *A*, the protocol for measuring unidirectional SR Ca efflux is shown. $^{45}$Ca uptake is started with the addition of ATP. Incubates were filtered at the indicated times to measure intravesicular Ca content. At 90 s, excess nonradioactive $^{40}$Ca buffered with 50 mM EGTA was added, diluting the $^{45}$Ca on the extravesicular (cytosolic) side of the membranes. This resulted in $^{45}$Ca efflux with $[Ca]_c$ maintained at 100 nM. The *points* are the individual time points (*i.e.* the raw data from a single experiment). The *black dashed line* indicates the theoretical steady-state $[Ca]_{SRT}$ ($^{45}$Ca + $^{40}$Ca). The *gray dashed line* is calculated from the leak data of Fig. 1. It is the estimated Ca that is lost because of leak (as opposed to pump reversal). Note the rapid loss of Ca compared with Fig. 1 indicating that the majority of this $^{45}$Ca efflux is pump-mediated backflux. *B*, balance of unidirectional Ca influx and efflux rates during net SR Ca uptake (for example as in *A*). Flux rates are calculated from the mean PLB-KO data (Fig. 3). Note that the efflux rate increases and the influx rate decreases as SR Ca content rises until these nearly balance and the net uptake rate becomes 0.

terize these experiments in a quantitative manner. Two different methods can be used to determine the SR Ca pump efficiency from the data. First previously determined SR Ca buffering characteristics (10) were used to convert vesicular $[Ca]_{SRT}$ to $[Ca]_{SR}$ (using Equations 12 and 13; see also Table II). Note that these values are similar to the 7000:1 $[Ca]_{SR}$:$[Ca]_c$ ratio (~700 $\mu$M $[Ca]_{SR}$) expected from the results of Shannon and Bers (10). From this ratio, the SR Ca pump efficiency was determined using Equations 1 and 2. We found a basal $\Delta G_{SRCa}$ in WT mice of 33.5 kJ/mol (56.8% efficiency). PLB-KO had a much higher $\Delta G_{SRCa}$ (43.9 kJ/mol; 74.5%). These results are summarized in the *top half* of Table II and graphically in Fig. 5.

Secondly, we used the measured uptake kinetics to calculate $\Delta G_{SRCa}$ in a different manner. We characterized the SR Ca uptake in terms of $V_{max}$, $K_{Ca-f}$, and $n$ in the forward direction from $J_{pumpf}$ (*i.e.* the initial uptake rate) as described under "Materials and Methods" (Table II). Similarly, backflux was also described assuming $V_{max} = V_{maxr}$ and $nf = nr$. Given $J_{pumpr}$ and the $V_{max}$ above, the $K_{Ca-r}$ was determined from Equation 8. Table II shows that the $K_{Ca-r}$ in PLB-KO is dramatically increased (1.401 *versus* 0.298 mM SR) consistent with the decreased rate of efflux observed in this phenotype.

If the initial uptake rate is lower in WT for the same $V_{max}$, $n$, and $[Ca]_c$, then $K_{Ca-f}$ must be higher. This will tend to reduce

and PLB-KO mice (33.5 kJ/mol, 56.8% and 43.9 kJ/mol, 74.5%, respectively). These results are summarized in the *top half* of Table II and graphically in Fig. 4, *C-E* and in Fig. 5.

## DISCUSSION

In the present study, we have provided the following new information: 1) passive leak from the SR with RyR (ryanodine receptors) blocked is small relative to backflux through the Ca pump, 2) passive leak from SR membranes is not PLB-dependent, 3) the efficiency of the Ca pump is decreased in the presence of PLB, and (4) PLB regulates this pump efficiency by decelerating influx while accelerating backflux through the SR Ca pump.

*Passive Ca Leak from SR Vesicles*—In all of the experiments presented, the SR RyR have been blocked with high (0.5 mM) concentrations of ryanodine. Under these conditions, only two efflux pathways are present, Ca efflux through the reverse mode of the SR Ca pump (Refs. 1–6, backflux) and passive Ca leak from the SR (which could in principal include flux via residual unblocked ryanodine receptors). To evaluate the backflux in our experiments, we first needed to make sure that leak would not interfere with our measurements to any significant extent.

We accomplished this by measuring the passive leak from the SR with both SR Ca pump influx and backflux blocked with thapsigargin (Fig. 1). SR Ca leak from the vesicles was less than 1% of our backflux measurements (Fig. 2) indicating that leak was a minimal amount of the total efflux and would not be expected to alter SR Ca content (9).

PLB coexists in the cardiac myocyte in both a monomeric and pentameric form (11, 24). The pentameric form might form a channel within the membrane and thus mediate SR Ca leak (12). We therefore measured leak in 3 different types of mice (PLB-70, PLB-C41F, and PLB-KO). The PLB-C41F group contained only mutant PLB, which does not form pentamers. The data showed no difference between the leak rates in PLB-70 and PLB-C41F (0.061 ± 0.010 *versus* 0.058 ± 0.011/min rate constants) indicating that the putative pentameric PLB channel did not conduct Ca under the conditions of our assay. Indeed, the leak rate from PLB-KO mice was not different from these two groups indicating that the presence or absence of SR PLB made no difference in our results for Ca leak. Thus our data do not provide support for a functionally relevant leak pathway created by PLB under our experimental conditions.

*SR Ca Pump Fluxes*—Forward and reverse fluxes are by definition equal and opposite at steady-state $[Ca]_{SRT}$ when leak is negligible. As uptake takes place and SR Ca accumulates, reverse pump-flux rate rises to meet the forward pump-flux rate (Fig. 2B). When leak is small (as it is here) the pump is expected to reach this point where the $[Ca]_{SR}/[Ca]_c$ gradient is at its thermodynamic limit. We found that $[Ca]_{SRT}$ rose exponentially to a steady-state value of $[Ca]_{SRT-SS}$ in WT, which was 22% of that in PLB-KO (Fig. 3). From this result, we suggest that PLB may lower the energetic efficiency of the SR Ca pump.

Consistent with this interpretation, kinetic analysis of the forward and reverse Ca pump flux indicated that the initial rate of uptake was higher in PLB-KO, whereas the rate of backflux at the same $[Ca]_{SRT}$ was lower. This implies a substantially lower $K_{Ca-r}:K_{Ca-f}$ ratio in WT, which would again imply lower $\Delta G_{SRCa}$ and energetic efficiency of the SR Ca pump in WT *versus* PLB-KO. In addition, the response to PLB appears to be graded with less of an effect in membranes from mice that have only 70% of the normal PLB levels (Fig. 4).

*Physiological and Pathophysiological Significance*—The decrease in SR Ca pump efficiency suggested here may have importance to both the understanding of normal physiology
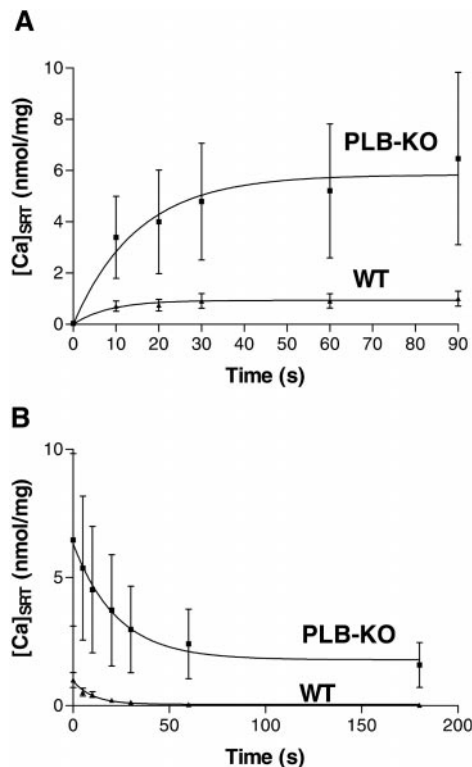


FIG. 3. **The figure shows the full time course of uptake (*A*) and efflux (*B*) experiments in WT and PLB-KO mice.** The assay is performed as in Fig. 2. WT mice took up Ca with a lower initial rate (0.13 *versus* 0.31 nmol/mg/s) to a lower steady-state $[Ca]_{SRT}$ (0.9 *versus* 4.1 nmol/mg protein). The efflux rate is higher in WT (0.065 *versus* 0.037 nmol/mg/s) at a $[Ca]_{SRT}$ of 0.8 nmol/mg. Data are mean ± S.E.; $n = 5–6$. The data are significantly different (two-way ANOVA, $p < 0.05$).

$\Delta G_{SRCa}$ according to Equation 11. Indeed initial uptake rates are lower in WT (0.13 *versus* 0.31 nmol/mg/s; see Fig. 3*A*), and this higher $K_{Ca-f}$ is consistent with extensive data on the effect of PLB on forward SR Ca pumping (21, 22).

Similarly for a given $V_{max}$, $[Ca]_{SRT}$, and $[Ca]_{SR}$ a higher rate of efflux in WT *versus* PLB-KO may be because of a lower $K_{Ca-r}$. A decreased $K_{Ca-r}$ in WT would also tend to reduce $\Delta G_{SRCa}$ (Equation 11). The rate of backflux at $[Ca]_{SRT} = 0.8$ nmol/mg was therefore evaluated using Equation 6 (Fig. 3*B*). Note that the rate of efflux is measured at 0.8 nmol/mg efflux-sensitive Ca (*i.e.* above the *plateau* in Fig. 3*B*). The rate of efflux in WT (0.065 nmol/mg/s) was higher than the rate of efflux in PLB-KO (0.037 nmol/mg/s). These results together with Equations 8 and 11 allows calculation of $\Delta G_{SRCa}$. The results are summarized in Table II. The values compare favorably with those determined by the first method above. Taken together the values are consistent with a PLB-dependent decrease in SR Ca pump efficiency (see Equation 1 and Fig. 5).

In addition, if the apparent decrease in SR Ca pump efficiency is because of the presence of PLB, we would predict that the response to phospholamban will be graded (*i.e.* the less PLB, the less the decrease in $E_{pump}$). The PLB-70 mice express PLB at 70% of the level seen in WT. This group shows SR Ca influx and backflux characteristics that fall between the PLB-KO and WT groups (Fig. 4). The initial rate of influx for PLB-70 was 0.17 with a backflux rate at 0.8 nmol/mg of 0.051 nmol/mg/s resulting in a $[Ca]_{SRT-SS}$ of 2.2 nmol/mg protein. All of these values fell between the values for PLB-KO and WT in Fig. 3.

Further analysis, as above for WT and PLB-KO, indicate a basal $\Delta G_{SRCa}$ in PLB-70 of 38.9 kJ/mol with 66.0% efficiency. These values are also intermediate between those of the WT

TABLE II

*SR Ca pump efficiency as determined from the SR [Ca] gradient and from the uptake kinetics, respectively*

The analysis assumes SR Ca buffering parameters from Shannon and Bers (10), $\Delta G_{ATP} = 59$ kJ/mol (13), and a Hill coefficient of 2. The $K_{Ca\text{-}f}$ values in the bottom part of the table are from Ref. 14. $V_{max}$ is calculated from the initial forward uptake rate. This same $V_{max}$ value is used to calculate $K_{Ca\text{-}r}$ from the rate of pump-mediated backflux. $\Delta G_{SRCa}$ is calculated using Equation 11.

| | Steady-state [Ca] gradient analysis | | | SR [Ca] gradient | $\Delta G_{SRCa}$ | Efficiency |
|---|---|---|---|---|---|---|
| Phenotype | $[Ca]_{SRT}$ | $[Ca]_{SRT}$ | $[Ca]_{SR}$ | | | |
| | *(nmol/mg)* | *(mmol/l SR)* | *(mmol/l SR)* | *($[Ca]_{SR}/[Ca]_c$)* | *(kJ/mol)* | *(%)* |
| WT | 0.9 | 1.82 | 0.09 | 900 | 33.5 | 56.8 |
| PLB-70 | 2.2 | 4.46 | 0.272 | 2720 | 38.9 | 66.0 |
| PLB-KO | 4.1 | 8.31 | 0.75 | 7500 | 43.9 | 74.5 |

| | Kinetic analysis | $K_{Ca\text{-}f}$ | $K_{Ca\text{-}r}$ | $K_{eq}$ | $\Delta G_{SRCa}$ | Efficiency |
|---|---|---|---|---|---|---|
| Phenotype | $V_{max}$ | | | | | |
| | *(nmol/mg/s)* | *(μM)* | *(mM)* | *($K_{Ca\text{-}r}/K_{Ca\text{-}f}$)* | *(kJ/mol)* | *(%)* |
| WT | 0.943 | 0.25 | 0.298 | 1193 | 34.9 | 59.1 |
| PLB-KO | 0.943 | 0.14 | 1.401 | 9800 | 45.3 | 76.7 |

FIG. 4. **The time course of uptake and efflux experiments in PLB-70 (70% of WT [PLB]) are demonstrated.** Data are mean ± S.E.; *n* = 3. The assay is performed as in Fig. 2. PLB-70 mice took up Ca with an initial influx rate of 0.17 nmol/mg/s to a steady-state $[Ca]_{SRT}$ of 2.2 nmol/mg protein. The efflux rate was 0.051 nmol/mg/s. This value is between the levels seen in WT and PLB-KO groups, indicating that the difference in $[Ca]_{SRT}$ is graded with PLB. *C*, *D*, and *E* summarize the results from *A* and *B* and from Fig. 3. $[Ca]_{SRT}$ is higher in PLB-KO (*C*) with a higher initial influx rate (*D*) and a lower efflux rate at 0.8 nmol/mg (*E*). PLB-70 is intermediate reflecting an intermediate [PLB]. These results indicate that PLB may decrease the efficiency of the SR Ca pump. Standard errors in *C* are for the plateau values in *A* and in Fig. 3*A* and are generated by the fitting program. All values in *C* are statistically different (one-way ANOVA).
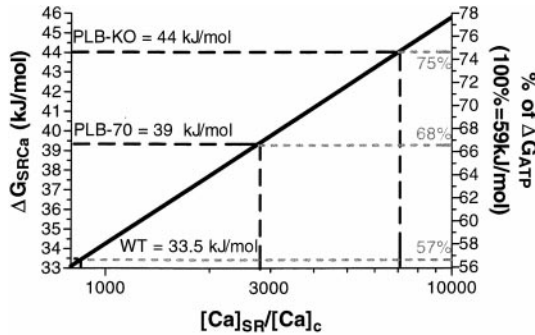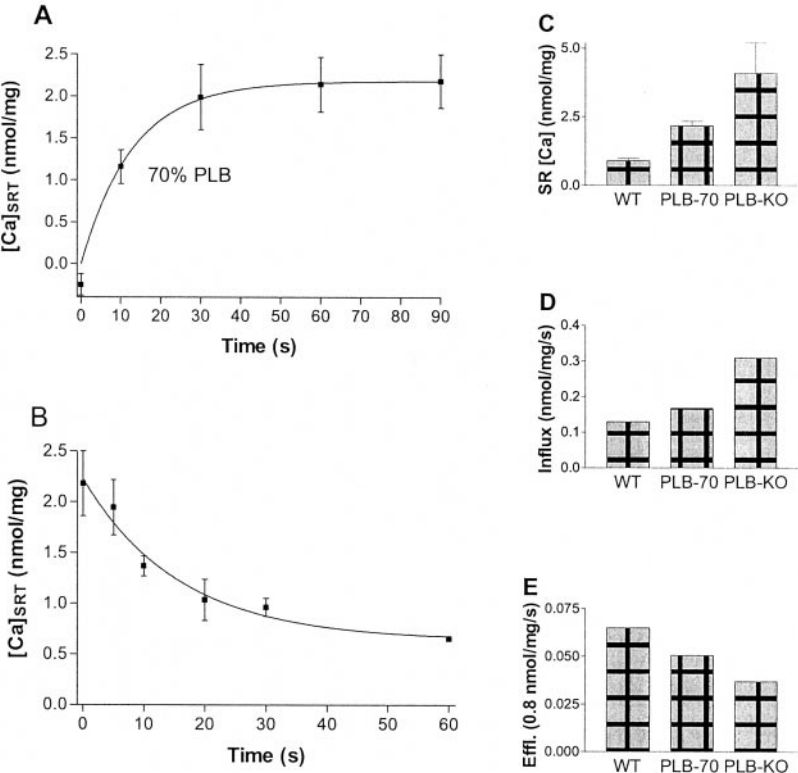
FIG. 5. **The figure demonstrates the efficiency of the SR Ca pump ± PLB.** $[Ca]_{SR}/[Ca]_c$ values are taken from Table II, and the *thick line* corresponding to $\Delta G_{SRCa}$ is based upon Equation 2. The *right ordinant* shows apparent energetic efficiency ($\Delta G_{SRCa}/\Delta G_{ATP}$; Equation 1) as a percent value.

and of cardiac disease states. Both in PLB-KO mice and when PLB is phosphorylated $[Ca]_{SRT}$ goes up (23). The increase in $[Ca]_{STR}$ leads to higher peak twitch $[Ca]_c$ both in part because

there is more Ca available for SR Ca release and because the fraction of that total SR Ca that is released rises (25–32).

The question of why $[Ca]_{SRT}$ goes up is a thorny one, however. It is well established that PLB phosphorylation increases the rate of SR Ca uptake and $[Ca]_c$ decline (7, 8, 21, 23). This has led to the hypothesis that diastolic $[Ca]_{SRT}$ increases simply because the SR Ca pump takes up more Ca in the given diastolic period. However, such an explanation presupposes that the Ca within the SR does not have time to approach a steady-state under normal physiological conditions and/or that the SR Ca pump balances a large SR Ca leak at rest. Though the pump is unlikely to reach a true thermodynamically limited gradient during the normal diastolic interval, data from our laboratory indicate that a large diastolic leak from the SR is unlikely (5, 6, 9, 33). If the pump efficiency was not changed, the PLB-dependent decrease in Ca uptake rate would cause $[Ca]_{SRT}$ to reach steady-state more slowly but would result in the same maximal $[Ca]_{SRT}$.

Our data here support the following alternative (though not mutually exclusive) hypothesis: that the decreased diastolic $[Ca]_{SRT}$ in WT is because of a decrease in the SR Ca pump

efficiency as defined by the steady-state SR [Ca] gradient. A reduced ability to generate such a gradient would naturally lead to a decrease in the steady-state SR Ca content. Our data indicate that such a mechanism is plausible and may contribute at least in part to the higher SR Ca accumulation typically observed in PLB-KO mice. In apparent contrast to this, isoproterenol treatment does not necessarily result in an appreciable increase in maximal $[Ca]_{SRT}$ (9). However, this result may be complicated by cAMP-dependent protein kinase effects on ryanodine receptors, causing an increased SR Ca leak via Ca release channels (34). Such a leak would tend to offset the ability of the pump to build a larger [Ca] gradient. This would also explain why blockage of the ryanodine receptors in isolated myocytes can sometimes lead to a much higher $[Ca]_{STR}$, especially in situations where higher SR Ca loads are favored (35). It would also promote increased SR Ca release as Ca sparks (36, 37).

In a concurrent study, Frank *et al.* (14) showed that PLB reduces the measured coupling ratio of the SR Ca pump (ratio of Ca taken up to ATP consumed) for $[Ca]_c$ at or below 300 nM (relevant to conditions here and physiological). How does the apparently lower stoichiometry from rate measurements relate to the present data and conclusions concerning thermodynamic efficiency? Their rate measurements were done in the virtual absence of Ca pump backflux, because they used oxalate to keep $[Ca]_{SR}$ from rising. Their complementary set of results may be another manifestation of the same depressant effect of PLB on SR Ca pump efficiency. A decline in coupling ratio means that one ATP cannot support transport of two Ca ions. This could mean that PLB allows the pump to slip backward more easily when $[Ca]_c$ is very low (without making ATP). In the present study this would show up as a lower limiting $[Ca]_{SR}/[Ca]_c$ gradient and lower energetic efficiency. Of course, this is speculative, and elucidation of the molecular mechanism for this apparent reduction in SR Ca pump efficiency by PLB will require further study.

By dissecting the effect into the component kinetic parameters, we can observe that the influx and efflux of Ca through the pump may both contribute their respective effects to the whole. This may become an important distinction when considering both pathological and pharmacological pump-associated phenomena. For instance, $\Delta G_{ATP}$ is decreased during ischemia, which may lead to a decrease in $[Ca]_{SRT}$. Increasing SR Ca pump efficiency in this situation may allow $[Ca]_{SR}$ and $[Ca]_c$ to remain relatively normal. Otherwise $[Ca]_{SR}$ would decline and $[Ca]_c$ would rise. This would reduce both systolic and diastolic function. Indeed the elevated $[Ca]_c$ may stimulate Ca-dependent proteases and lead to mitochondrial Ca loading, both of which can lead to cell death.

The data may also give us a better understanding of cardiac disease states where the PLB:SR Ca pump ratio may be increased (as reviewed by Koss *et al.* (38)). Such an increase would result in decreased SR Ca not only because of reduced pump rate (reducing the chances of reaching diastolic SR steady-state) but also because the ability of the pump to build the normal $[Ca]_{SR}/[Ca]_c$ gradient would be reduced. Given this, increasing not only the rate but the efficiency of the pump may be especially important in both physiologic responses, as well as therapeutics.

In summary, we have measured the parameters for SR Ca efflux both through the SR Ca pump and through passive SR Ca leak. Though we found no PLB-dependent increase in the leak rate, a PLB-dependent increase in SR Ca backflux through the SR Ca pump is apparent. This increased backflux contributes to an apparent decrease in SR Ca pump efficiency, which may be important in both pathophysiological and physiological states.

## REFERENCES

1. Feher, J. J., and Briggs, F. N. (1984) *Biophys. J.* **45,** 1135–1144
2. Takenaka, H., Adler, P. N., and Katz, A. M. (1982) *J. Biol. Chem.* **257,** 12649–12656
3. Weber, A., Herz, R., and Reis, I. (1966). **345,** 329–369
4. Makinose, M. (1971) *FEBS Lett.* **12,** 269–270
5. Shannon, T. R., Ginsburg, K. S., and Bers, D. M. (1997) *Ann. N. Y. Acad. Sci.* **853,** 350–352
6. Shannon, T. R., Ginsburg, K. S., and Bers, D. M. (2000) *Biophys. J.* **78,** 322–333
7. Kranias, E. G. (1985) *Biochim. Biophys. Acta* **844,** 193–199
8. Tada, M., Inui, M., Yamada, M., Kadoma, M. A., Kuzuya, T., Abe, H., and Kakiuchi, S. (1983) *J. Mol. Cell. Cardiol.* **15,** 335–346
9. Ginsburg, K. S., Weber, C. R., and Bers, D. M. (1998) *J. Gen. Physiol.* **111,** 491–504
10. Shannon, T. R., and Bers, D. M. (1997) *Biophys. J.* **73,** 1524–1531
11. Wegener, A. D., and Jones, L. R. (1984) *J. Biol. Chem.* **259,** 1834–1841
12. Kovacs, R. J., Nelson, M. T., Simmerman, H. K. B., and Jones, L. R. (1988) *J. Biol. Chem.* **263,** 18364–18368
13. Allen, D. G., Morris, P. G., Orchard, C. H., and Pirolo, J. S. (1985) *J. Physiol.* **361,** 185–204
14. Frank, K., Tilgmann, C., Shannon, T. R., Bers, D. M., and Kranias, E. G. (2000) *Biochemistry,* **39,** 14176–14182
15. Grynkiewicz, G., Poenie, M., and Tsien, R. Y. (1985) *J. Biol. Chem.* **260,** 3440–3450
16. Bers, D. M., Patton, C. W., and Nuccitilli, R. (1994) *Methods Cell Biol.* **40,** 3–29
17. Hove-Madsen, L., and Bers, D. M. (1993) *Am. J. Physiol.* **264,** C677-C686
18. Page, E., Mccallister, L. P., and Power, B. (1971) *Proc. Natl. Acad. Sci.* **68,** 1465–1466
19. Page, E. (1978) *Am. J. Physiol.* **235,** C147-C158
20. Sagara, Y., Wade, J. B., and Inesi, G. (1992) *J. Biol. Chem.* **267,** 1286–1292
21. Chu, G., Li, L., Sato, Y., Harrer, J. M., Kadambi, V. J., Hoit, B. D., Bers, D. M., and Kranias, E. G. (1998) *J. Biol. Chem.* **273,** 33674–33680
22. Luo, W., Grupp, I. L., Harrer, J., Ponniah, S., Grupp, G., Duffy, J. J., Doetschman, T., and Kranias, E. G. (1994) *Circ. Res.* **75,** 401–409
23. Li, L., Chu, G., Kranias, E. G., and Bers, D. M. (1998) *Am. J. Physiol.* **274,** H1335-H1347
24. Koss, K. L., and Kranias, E. G. (1996) *Circ. Res.* **79,** 1059–1063
25. Isenberg, G., and Han, S. (1994) *J. Physiol.* **480,** 423–438
26. Bassani, J. W. M., Yuan, W., and Bers, D. M. (1995) *Am. J. Physiol.* **268,** C1313-C1329
27. Spencer, C. I., and Berlin, J. R. (1995) *J. Physiol.* **488,** 267–279
28. Spencer, C. I., and Berlin, J. R. (1997) *J. Physiol.* **504,** 565–578
29. Santana, L. F., Kranias, E. G., and Lederer, W. J. (1997) *J. Physiol.* **503,** 21–29
30. Dettbarn, C., and Palade, P. (1997) *Mol. Pharmacol.* **52,** 1124–1130
31. Hüser, J., Bers, D. M., and Blatter, L. A. (1998) *Am. J. Physiol.* **274,** H1800-H1811
32. Shannon, T. R., Ginsburg, K. S., and Bers, D. M. (2000) *Biophys. J.* **78,** 334–343
33. Bassani, R. A., and Bers, D. M. (1995) *Biophys. J.* **68,** 2015–2022
34. Marx, S. O., Reiken, S., Hisamatsu, Y., Jayaraman, T., Burkhoff, D., Rosemblit, N., and Marks, A. R. (2000) *Cell* **101,** 365–376
35. Overend, C. L., Eisner, D. A., and O'Neill, S. C. (1997) *J. Physiol.* **502,** 471–479
36. Cheng, H., Lederer, W. J., and Cannell, M. B. (1993) *Science* **262,** 740–744
37. Satoh, H., Blatter, L. A., and Bers, D. M. (1997) *Am. J. Physiol.* **272,** H657–668
38. Koss, K. L., Grupp, I. L., and Kranias, E. G. (1997) *Basic Res. Cardiol.* **92,** Suppl. 1, 17–24
39. Feher, J. J., and Briggs, F. N. (1982) *J. Biol. Chem.* **257,** 10191–10199
40. Post, J. A., and Langer, G. A. (1992) *J. Membr. Biol.* **129,** 49–57
41. Bers, D. M., Allen, L.-A. H., and Kim, Y.-J. (1986) *Am. J. Physiol.* **251,** C861-C871
42. Martell, A., and Smith, R. M. (eds) (1974) *Critical Stability Constants*, pp. 269–272, Plenum Publishing Corp., New York
43. Jackson, A., Timmerman, M., Bagshaw, C., and Ashley, C. (1987) *FEBS Lett.* **216,** 35–39

**Phospholamban Decreases the Energetic Efficiency of the Sarcoplasmic Reticulum Ca Pump**

Thomas R. Shannon, Guoxiang Chu, Evangelia G. Kranias and Donald M. Bers

Access the most updated version of this article at doi: 10.1074/jbc.M007085200

Alerts:
- When this article is cited
- When a correction for this article is posted

Click here to choose from all of JBC's e-mail alerts

This article cites 41 references, 13 of which can be accessed free at
http://www.jbc.org/content/276/10/7195.full.html#ref-list-1